Atmospheric Pollution Research 6 (2015) 415-427

Atmospheric Pollution Research

www.atmospolres.com

Inspection of high–concentration CO_2 events at the Plateau Rosa Alpine station

Silvia Ferrarese [1], Francesco Apadula [2], Fabio Bertiglia [1], Claudio Cassardo [1], Andrea Ferrero [1], Lucio Fialdini [2], Caterina Francone [1], Daniela Heltai [2], Andrea Lanza [2], Arnaldo Longhetto [1], Massimiliano Manfrin [1], Renzo Richiardone [1], Claudio Vannini [2]

[1] *Department of Physics, University of Torino, via P. Giuria 1, 10125, Torino, Italy*
[2] *Ricerca sul Sistema Energetico–RSE, via R. Rubattino 54, 20134, Milano, Italy*

ABSTRACT

The Plateau Rosa Alpine station (Italy) has collected atmospheric concentrations of carbon dioxide since 1989. If the complete set of hourly data is observed, two distinct and exceptional very high concentration events are evident for February 2004. Similar and almost contemporary peaks were registered at the European high–altitude stations of Zugspitze–Schneefernerhaus and Sonnblick in the Alps, and at Mt. Cimone in the Northern Apennines. A regional meteorological model (the Weather Research and Forecast) was applied over a medium–high resolution grid to study the evolution of the meteorological fields and to identify the trajectories of the polluted air masses during the CO_2 observed peaks. The results show that, during both episodes, atmospheric circulation conveyed highly polluted air from the European plains to the Alpine stations. This conclusion has been also confirmed through concentration measurements of the atmospheric trace gases in the same area.

Keywords: *Air trajectory, CO_2 atmospheric concentration, Plateau Rosa station, WRF model*

Corresponding Author:
Silvia Ferrarese
☎ : *+39-011-6707441*
🖷 : *+39-011-6707020*
✉ : *silvia.ferrarese@unito.it*

Article History:
Received: 22 July 2014
Revised: 05 November 2014
Accepted: 17 November 2014

doi: 10.5094/APR.2015.046

1. Introduction

Increases in atmospheric carbon dioxide concentrations are of considerable concern as far as global climatic changes are concerned, due to its Greenhouse Warming Potential (GWP, Lashof and Ahuja, 1990). The monitoring of atmospheric CO_2 began in 1958 at the Mauna Loa Observatory in Hawaii (Keeling et al., 1976; Keeling, 2008), and in the following years a growing number of monitoring stations started their measurements in different parts of the world. In order to create a reliable and complete data network of CO_2 and other greenhouse gas concentrations, the World Meteorological Organization (WMO) established the Global Atmosphere Watch (GAW) program in 1991, which actually involves about 80 countries. As part of the GAW program, the World Data Centre for Greenhouse Gases (WDCGG), hosted by the Japanese Meteorological Agency, collects and distributes greenhouse gas concentration data. The GAW program has the aim of providing data and information on the chemical composition of the atmosphere, as well as of improving the understanding of the changes in concentration of natural and anthropogenic gases and the mutual interactions between atmosphere, oceans and biosphere.

The original aim of monitoring CO_2 was to evaluate its global background concentration and rate of increase (Conway et al., 1988; Conway et al., 1994). Recently, CO_2 datasets have also been used for other purposes, such as the study of net ecosystem exchanges (Peters et al., 2010), and of the latitudinal and seasonal patterns of sources and sinks and their magnitudes (Tans et al., 1989; Rodenbeck et al., 2003).

Among the hundreds of GAW stations that measure CO_2 concentrations, only the background ones, i.e. those located far from local sources and sinks, can be considered suitable to perform global analyses of atmospheric background concentrations (Conway et al., 1994; Masarie and Tans, 1995). The hourly data collected at these stations is filtered with different techniques, which depend on the particular features of the station, to eliminate the influence of any eventual local or regional transport features. The filtered CO_2 concentration data, which are averaged on a monthly basis, are then elaborated to calculate the global CO_2 trend in the atmosphere (WMO, 2009). This procedure implies that short episodes of high or low concentrations, probably connected to local or regional transport events, are eliminated from the background data.

Complete sets of unfiltered data are used in data assimilation techniques to estimate the net ecosystem exchange (Peters et al., 2010) and inverse models to localize source and sink areas (Bousquet et al., 2000; Rodenbeck et al., 2003). In such studies, high–frequency data are needed to capture the variability of the observations. Single events with anomalous values of CO_2, if measured at sites far from source areas, are useful to know the concentration variability (Wada et al., 2007).

In the Alps, a few high altitude stations, located at more than 2 000 m a.s.l., measure the background concentrations of CO_2. Their measurements are useful to evaluate the interannual CO_2 trend over the European continent (Apadula et al., 2003; Schoner et al., 2012). Episodically, these stations also record high concentration peaks, which, because of their amplitude, do not fall into the typical daily cycle (Apadula et al., 2003; Uglietti et al., 2011). These peaks can originate from local effects and/or from synoptic scale transport.

In such a complex orographic environment, mountain venting influences the measurements (Kossmann et al., 1999). This process occurs in fair weather during the day, when mountain induced updrafts are able to vertically cross the capping inversion, thus favoring an exchange between the atmospheric boundary layer and the free troposphere. Mountain venting was initially described by Kossmann et al. (1999), who detected an at least 500 m high plume between the boundary layer and the free troposphere over the Black Forest (Germany). Mountain venting in the Alpine environment was also studied in depth in other experimental studies (Henne et al., 2004; Henne et al., 2005a; Henne et al., 2005b; Gohm et al., 2009) and in numerical simulations (Weigel et al., 2007).

As far as the correlation between the CO_2 concentrations at Alpine stations and long–range transport is concerned, it has been shown that the measurement of non–fully mixed air masses at the Plateau Rosa station (Italy) could be related to atmospheric circulation patterns (Longhetto et al., 1995; Longhetto et al., 1997). Apadula et al. (2003) described an episode of a high CO_2 concentration measured at the Plateau Rosa and Zugspitze (Germany) Alpine stations and showed that the same air masses reached Plateau Rosa and then Zugspitze 12 to 18 hours later. Uglietti et al. (2011) have recently analyzed two high CO_2 level events at the Jungfraujoch station (Switzerland), and have investigated the source areas on a synoptic scale.

In the present paper, two consecutive very high CO_2 concentration events have been identified in the unfiltered hourly data records of four European high altitude stations, and in particular at the Plateau Rosa station, where the maximum concentration was observed.

In the past, the CO_2 concentrations at Plateau Rosa were analyzed using backward trajectories that were calculated by interpolating the wind speed air fields from global models (resolution of 0.5x0.5 degrees in latitude and longitude). Cluster analysis (Longhetto et al., 1995; Longhetto et al., 1997) and a trajectory statistical method (Ferrarese et al., 2002; Apadula et al., 2003) were applied to identify the meteorological patterns and the source areas connected to high CO_2 values, respectively.

In this paper, the two events have been studied by means of 7 km resolution model to deduce the path of the air trajectories and estimate the origin of the contamination. The model has been validated through a comparison with the measured data, and some measurements of pollutant gases over the European area have been used in order to confirm the obtained results.

2. Measurements

Two high CO_2 concentration events were observed in February 2004 at the remote site of Plateau Rosa (Italy). In order to exclude the presence of local effects, CO_2 concentrations measured in the same period at other European background stations located at altitudes above 2 000 m a.s.l. and which can be found in the WDCGG database, were analyzed. The selected stations are Zugspitze–Schneefernerhaus (Germany), Sonnblick (Austria) and Mt. Cimone (Italy). Their geographical positions (Zugspitze–Schneefernerhaus and Sonnbick on the northern side of the Alps and Mt. Cimone on the northern Apennines) allow CO_2 concentrations to be monitored around the Alps (Figure 1).

2.1. The monitoring stations

The Plateau Rosa station (GAW Identification Code: PRS, latitude: 45.93°N, longitude: 7.71°E, altitude: 3 480 m a.s.l.) is one of the highest European atmospheric monitoring stations: it is located on the Italian side of the Alps (Figure 1), near the Mt. Cervino (also known as Matterhorn). The station is located at a typical elevation of the free atmosphere upon a large snow–clad bare mountain plateau and far from urban and polluted zones. Owing to its high altitude and position, it is suitable for the background measurement of greenhouse gases. A nearby meteorological station measures the air temperature, relative humidity, pressure and wind (speed and direction). The main greenhouse gases (carbon dioxide, methane, and ozone) at the PRS station are measured regularly by the Ricerca sul Sistema Energetico (RSE) team.

The PRS CO_2 dataset currently covers 25 complete years. The atmospheric CO_2 concentration, referring to the WMO X2007 international mole fraction scale, is measured by means of a continuous non–dispersive infrared analyzer (ULTRAMAT 5E and 6E) working in the 350–400 ppm (5E) and 360–410 ppm (6E) ranges, respectively. Hereafter, the CO_2 ppm units stand for micromoles/mol dry air. The monitoring frequency is 0.5 Hz and the data were averaged every 30 minutes until 2007, and then every 60 minutes to be consistent with international measurement standards. The estimated measurement standard uncertainty is about 0.07 ppm.

The long–term CO_2 record has been used to evaluate interannual and decadal changes in the atmospheric CO_2 concentration gradient in Europe (Ramonet et al., 2010) and to validate of atmospheric greenhouse gas models (Trusilova et al., 2010) and inverse source–receptor models (Geels et al., 2007).

The historical series of the monthly CO_2 background concentrations was obtained by applying a filtering scheme. The long–term trend and seasonal oscillation that were induced by the vegetation cycle, from March 1993 to December 2013 can be observed in Figure S1 (see the Supporting Material, SM). The linear trend over the whole period is equal to 1.98 ± 0.04 ppm/year, and is comparable with the value of the global trend (1.91 ppm/year) computed for the years 1995–2005 by IPCC (Forster et al., 2007) and about 2.0 ppm/year (for the last decade) reported in the WMO Greenhouse Gas Bullettin (WMO Greenhouse Gas Bulletin, 2013).

The Zugspitze–Schneefernerhaus station (GAW ID: ZSF) is located in the German Alps (47.42°N, 10.98°E, 2 656 m a.s.l., Figure 1). This station measures concentrations of methane, carbon monoxide, carbon dioxide, nitrogen oxides, ozone, and sulfur hexafluoride. The Sonnblick station (GAW ID: SNB, 47.05°N, 12.95°E, 3 106 m a.s.l.) is located in the Austrian Alps (Figure 1) and measures atmospheric concentrations of carbon monoxide, carbon dioxide (since 1999), ozone, and nitrogen oxides. The Mt. Cimone station (GAW ID: CMN, 44.18°N, 10.70°E, 2 165 m a.s.l.) is located in the Northern Italian Apennines (Figure 1) where it measures concentrations of methane, carbon monoxide, carbon dioxide, hydrogen and ozone. The atmospheric CO_2 record from Mt. Cimone dates back to 1979 and represents the longest, continuous historical series available in the Mediterranean area. The CO_2 concentration values used in this study and the information about the above mentioned stations are available on the WDCGG website (WDCGG, 2014).

2.2. The two extreme CO_2 concentration events

At PRS site, the frequency distribution of the differences between the daily mean values and the corresponding monthly averages of the CO_2 concentration computed over 21 years (from 1993 to 2013), shows an upper tail of values greater than 3σ composed by 51 cases over more than 6 000 days, the standard deviation σ being equal to 1.7 ppm. They are much more frequent

in winter (47%) and in autumn (33%) than in spring (18%) and summer (2%), probably due to higher emissions and atmospheric stability during the cold season. Four episodes can be considered exceptional (values greater than 6σ). Two of them occurred in autumn (November, 2003 and October, 2007) and two very close in winter (on 19 and 23 February 2004). The two subsequent events of February, 2004 are characterized by the highest absolute concentrations and are analyzed in detail in the present study.

Observing the 30–minute unfiltered CO_2 concentration data measured during the second half of February 2004 at PRS, the two consecutive higher events than 400 ppm, i.e. about 20 ppm more than the usual value for that period, are evident (Figure 2). During the first event, which lasted 48 hours, the CO_2 concentration values started to rise on 18 February at 13:00 UTC and reached a first peak at 22:00 UTC, a second peak of about 401 ppm (absolute maximum) on 19 February at 06:00 UTC, a third peak at 12:00 UTC, and finally decreased slowly until the evening of 20 February, when the event terminated. The second event lasted 22 hours, from 04:30 UTC on 23 February to 02:30 UTC on 24 February, and showed a single isolated peak of about 408 ppm on 23 February at 15:30 UTC.

A comparison between the concentrations measured in the four sites during the period from 17 to 25 February 2004 shows that very high values were also measured at the two Zugspitze–Schneefernerhaus (ZFS) and Sonnblick (SNB) Alpine remote stations, as well as at Mt. Cimone (CMN) (Figure 2). The ZFS station registered the onset of the first event at 01:00 UTC on 18 February (twelve hours earlier than PRS), two peaks at 23:00 UTC on 18 February and at 09:00 UTC on 19 February with intensities comparable to those measured at PRS, and the events ended at the same time. Unfortunately, the second event was only partially detected, due to a lack of data from the evening of 21 February to the morning of 23 February (Figure 2a). The SNB station also measured the first event, and showed similar intensity and timings as PRS (Figure 2b). The event started at 07:00 UTC on 18 February, and two peaks were detected at 20:00 UTC on 18 February and at 07:00–08:00 UTC on 19 February. Although the second event was clearly visible, its maximum appeared to be lower and there were also scattered, moderately high values on 22 and 24 February (Figure 2b). High concentrations were also measured at the CMN station during both episodes, but they showed lower maxima and were delayed by several hours (Figure 2c). The maximum values were reached for the first and the second event at 10:00 UTC on 20 February and at 07:00 UTC on 24 February, respectively.

Figure 3 shows the distribution of the differences between the daily and the monthly averages in the years from 2002 to 2006 at the four Alpine stations. The differences at PRS surpassed 6σ in both February 2004 episodes, whereas they ranged between σ and 3σ in the other stations. Thus, the intensities of the CO_2 peaks measured at the ZSF, SNB and CMN stations are statistically more likely to occur.

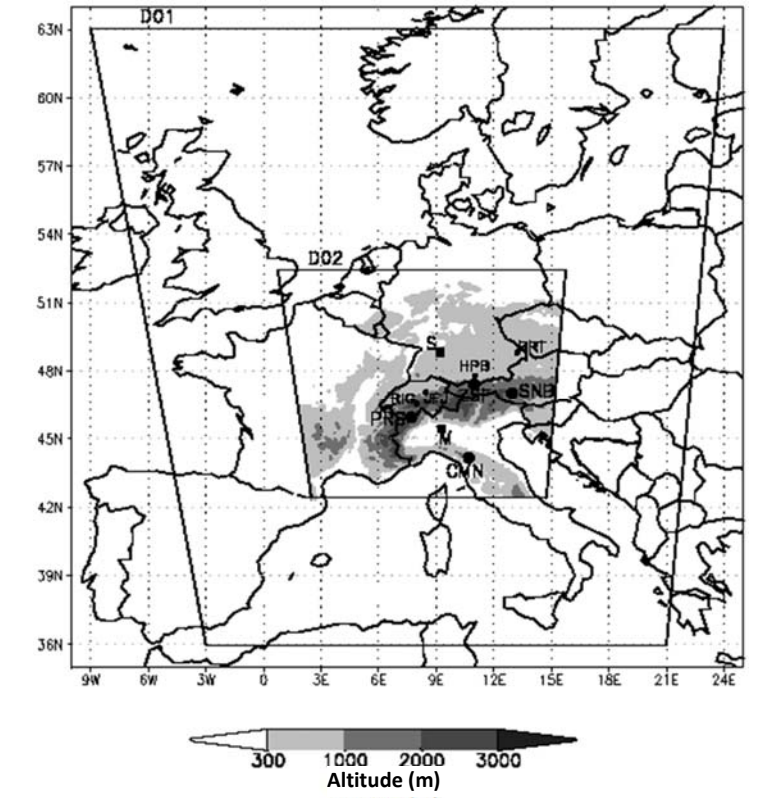

Figure 1. *Geographical sites of the Plateau Rosa (PRS), Sonnblick (SNB), Zugspitze–Schneefernerhaus (ZFS) and Mt. Cimone (CMN) CO_2 monitoring stations (points), the Brotjacklriegel (BRT), Hohenpeissenberg (HPB), Jungfraujoch (JFJ), and Rigi (RIG) CO and/or O_3 monitoring stations (small points), the Milan (M) and Stuttgart (S) radio–sounding stations (squares). The two boxes delineate the two WRF domains: D01 is the parent grid (21 km resolution) and D02 is the nested grid (7 km resolution). The terrain altitude (m) is shaded in the D02 domain (white: under 300 m, light grey: between 300 m and 1 000 m, medium grey: between 1 000 m and 2 000 m, dark grey: between 2 000 m and 3 000 m, black: above 3 000 m).*

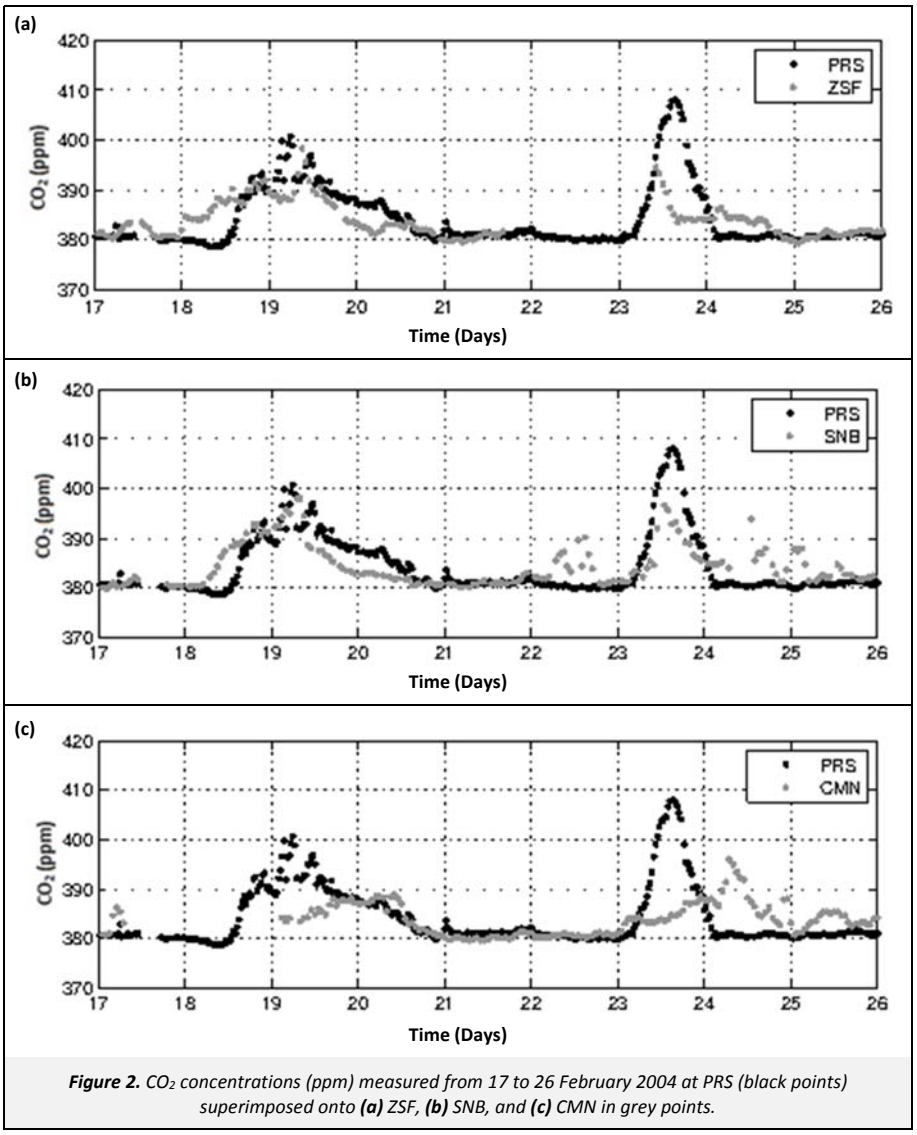

Figure 2. *CO_2 concentrations (ppm) measured from 17 to 26 February 2004 at PRS (black points) superimposed onto* ***(a)*** *ZSF,* ***(b)*** *SNB, and* ***(c)*** *CMN in grey points.*

The similar behavior of the CO_2 data collected at the four stations suggests that the investigated episodes were probably connected to mesoscale or synoptic features, even though the exceptional concentration levels measured at the PRS station could suggest an additional contribution from a local or regional source. In order to study a probable link with polluted episodes, the concentration of short–lived gases (carbon monoxide and ozone) during the same periods at the GAW stations in the studied area are examined in Section 5.

3. Meteorological Background

An inspection of surface meteorological maps and 500 hPa level geopotential reanalyses has shown that the synoptic situation during the first eighteen days of February 2004 was predominantly characterized by sub–tropical anticyclonic structures over the Mediterranean and central European areas. This meteorological situation causes the presence of inversions, with frequent episodes of fog and low–level stratified clouds over the plains. This situation can also be confirmed by looking at the radiosoundings registered at the Milan station, which is representative of the Po Valley, and the Munich and Stuttgart stations, which are representative of the Northern side of the Alps (not shown).

On 18 February (see the SM, Figure S2a), the intensification of the anticyclone over the UK and a depression that moved from the Norwegian Sea towards S–SE advected air masses from the north–east Atlantic towards central Europe. On 19 February, the surface map (Figure S2b) showed the formation of a cyclogenesis on the Ligurian Sea with two associated fronts, one cold in the western side and another warm in the eastern side. The warm front moved northwards and crossed the entire Po Valley, approaching the Southern Alps during the early morning of 19 February. Subsequently, the structure evolved and the frontal systems occluded. This event caused rainy and snowy conditions over Po Valley, with a northern wind blowing through the Alps and the North Adriatic basin being affected by an episode of Bora wind.

On 20 February, the frontal system moved slowly from Northern Italy towards the East and a new, deep depression developed in the South–western part of the Iberian Peninsula. In the following days, this depression moved eastwards, with its frontal systems inducing a strong flow towards central Europe (south–westerly at upper levels and south–easterly at sea level). As a consequence, the Northern Adriatic area was affected by an episode of Sirocco wind that lasted until 22 February.

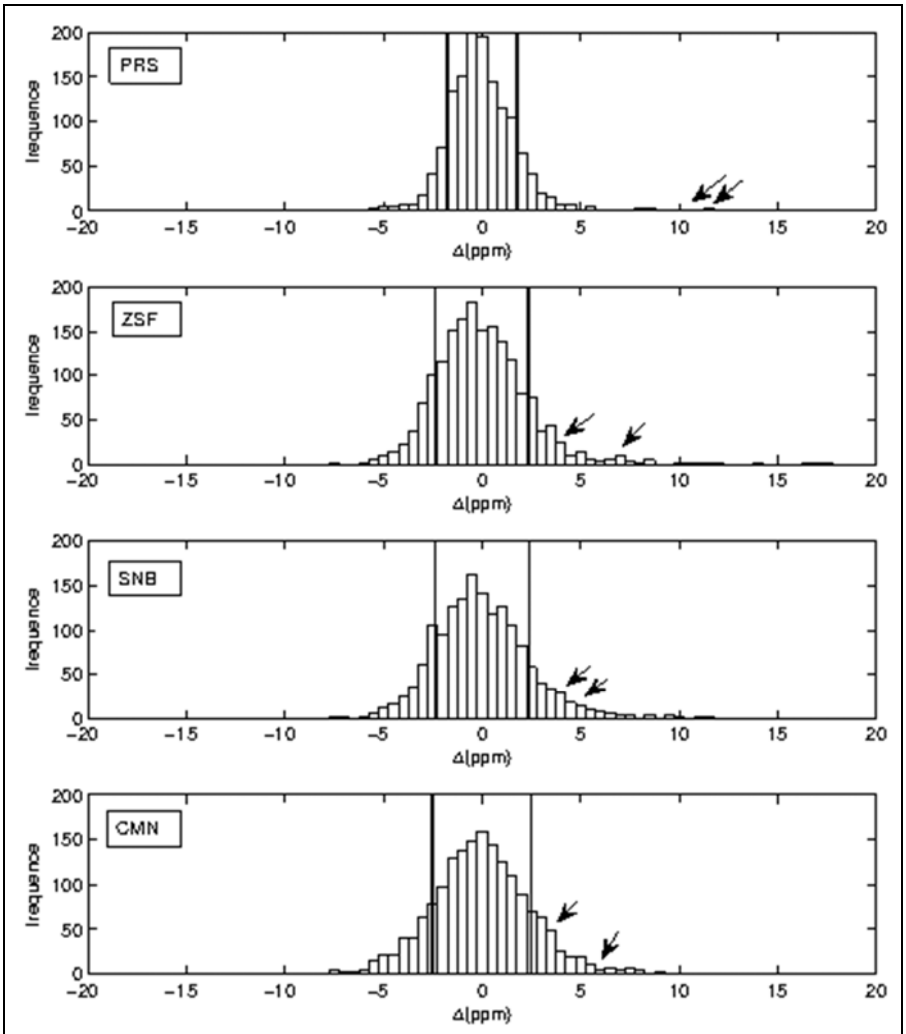

Figure 3. *Distribution of the differences [Δ(ppm)] between the daily and monthly averages of CO_2 concentrations at PRS, ZSF, SNB and CMN computed over the 2002–2006 period. The vertical lines indicate the ±σ interval. The values related to the two episodes fall into the bins highlighted by the two arrows.*

The frontal system from the Iberian Peninsula reached the Western side of Italy on 22 February in the evening (see the SM, Figure S2c) and on 23 February, a minimum developed over the Ligurian Sea (Figure S2d). The cold air associated with the cold front crossed the Alps in the morning of the 23 February; subsequently, during 24 February, the depression moved away and the winds weakened.

Due to the complexity of the meteorological situations, the descriptions, which were provided by the maps every 12 or 24 hours, are not sufficiently accurate to explain in detail the paths of the air masses. For this reason, the application of a high resolution meteorological model is necessary.

4. WRF Model

4.1. The WRF model: a brief description

In order to study the air trajectories during the two episodes and to investigate the high CO_2 concentration source regions, the WRF (Weather Research and Forecasting) atmospheric model was used. This is a mesoscale numerical weather prediction model that has been designed to carry out both operational forecasting and atmospheric research. WRF is a fully compressible, non–hydrostatic, primitive–equation model with multiple–nesting capabilities which can enhance resolution over the areas of interest. WRF offers several options for parameterize: microphysics, long and short wave radiation, surface layer physics, boundary layer physics and cloud physics.

WRF has been developed through a collaborative partnership between the National Center for Atmospheric Research (NCAR), the National Oceanic and Atmospheric Administration (NOAA) and more than one hundred research centers and universities. It is maintained and supported as a community model and is adopted by many meteorological offices. A detailed description of the equations, physics and dynamics of the model is available in Skamarock et al. (2008).

Among the recent studies that have reported WRF simulations in European complex orography conditions, Papanastasiou et al. (2010) have analyzed the wind field over the east coast of central Greece in typical summer conditions, Mastrangelo et al. (2011) have investigated a heavy precipitation event that occurred in South–eastern Italy, Miglietta et al. (2011) have analyzed different simulations of a Mediterranean 'hurricane', Trapero et al. (2013) have examined the effects of orography on two heavy precipitation events in the Eastern–Pyrenees in the Northwest Mediterranean, and Miglietta et al. (2013) have studied two cases of intense lee waves in the Eastern Mediterranean Sea.

4.2. WRF configuration

An 11–day simulation was carried out from 15 to 25 February 2004 with WRF (version 3.0) in order to study the wind patterns before and during the two CO_2 concentration peaks, with the aim of reconstructing the air trajectories and of investigating the contribution of the polluted air masses.

Two nested grids with 28 vertical levels were arranged using the two–way grid configuration (Figure 1). The parent grid covers the whole of central Europe, and extends partially over Northern Europe and the Western Mediterranean Sea, and has a 21 km horizontal resolution. The nested grid, with a 7 km horizontal resolution, includes the PRS, CMN, ZFS and SNB stations, and it covers central Europe, the Alps, and northern and central Italy.

The static data of the surface elevation and land use, which were available at 10' and 2' resolutions, were used to characterize the lower initial and boundary conditions in the parent and inner domains, respectively. The model topography is smoothed: in the inner domain (Figure 1), the highest peak in the Alps reaches an altitude of 3 100 m at the Monte Rosa Massif position (latitude: 45.9°N, longitude: 7.8°E). Six–hour ECMWF analyses conducted on the surface and on 11 pressure levels (1 000, 925, 850, 700, 500, 400, 300, 250, 200, 150 and 100 hPa), and with a horizontal grid resolution of 0.5°x0.5° in latitude and longitude, were used as the initial and boundary conditions.

The WRF time step was set to 2 minutes for the parent grid and 40 seconds for the nested grid, and the output data were stored every 3 hours. The schemes selected for the microphysics, planetary boundary layer, surface processes, radiation and clouds are listed in Table 1.

Table 1. *Parameterizations selected in the WRF options*

Physics Categories	Scheme
Microphysics	Purdue Lin
Long wave radiation	RRTM
Short wave radiation	MM5 (Dudhia)
Surface layer	Similarity theory (MM5)
Land–surface model	5–layers thermal diffusion
Planetary boundary layer	YSU
Cumulus parameterization	Kain–Fritsch

Finally, the RIP4 (Read Interpolate Plot version 4, Stoelinga, 2009) post processor was used to calculate the three–dimensional backward air trajectories from the WRF output in the inner domain.

4.3. Model evaluation

In order to validate the model performance, the vertical profiles of the simulated wind speeds, directions and temperatures from the inner grid domain were compared with some radiosonde observations. Despite the limited number of stations, this kind of comparison is better than only using ground observations because it allows the simulated values in the whole atmospheric profile to be evaluated. The vertical profiles of the simulated wind directions, wind speeds and temperatures from the fine grid domain were compared with radiosoundings from both sides of the Alps: Milan (Italy) and Stuttgart (Germany) (Figure 1).

For the first event, which featured intense winds over the Po Valley, the comparison was made on the Southern side of the Alps (see the SM, Figure S3). A qualitative agreement of the modeled wind and temperature profiles with radiosonde data can be observed. In particular, the air mass advection from the East, below the 800 hPa level, was captured well for both the directions and speeds (Figures S3a and S3b). The root mean squared error (RMSE) between the simulated and observed values was 3.3 m/s for the wind speed and 17 degrees for the direction in the troposphere under the 800 hPa level. The agreement is much lower in the 750–400 hPa layer, but this does not influence the trajectory of the air parcels arriving at PRS station (Section 4).The temperature was modeled well throughout the whole profile (Figure S3c) and in particular in the layer below 800 hPa, where the RMSE value was 1.4 °C.

For the second event, when a North wind blew towards the Alps, the comparison was made for the northern side of the Alps (Figure S4). Here, WRF captured the de–coupling between the northern flow below the 800 hPa level and the westerly circulation above. This de–coupling was marked by a strong inversion that prevented vertical mixing between the boundary layer and the upper atmosphere. This condition suggests the advection of highly polluted air towards the Alps. The RMSE values were 17 degrees for wind direction, 2.9 m/s for wind speed, and 1.1 °C for temperature in the layer below 800 hPa.

5. Results and Discussion

In order to examine the air flow during each episode and to identify the origin and path followed by the air masses arriving at the remote stations, the wind speed fields computed by the WRF model and the three–dimensional trajectories have been analyzed in this section.

In the inner domain, the three–dimensional trajectories were computed in backward mode every three hours. Their maximum length was set to two days. As far as the applicability of the calculated trajectories is concerned, position errors depends mainly by the spatial and temporal resolution of the wind field (Bowman et al., 2013), but the choice of the height of the trajectory destination was a major problem, because the model topography was lower and smoother than the real one. Wotawa et al. (2000) and Loov et al. (2008) used the real height of a station as the point of arrival because they were interested in large–scale flows. Kaiser et al. (2007) chose an altitude close to that of the model, because they studied the transport from polluting sources close to the surface, whereas Uglietti et al. (2011) decided on an intermediate value between the real and the modeled topography. In this work, the trajectory destination was fixed at the model surface as in Kaiser et al. (2007): it was set to 2 934 m a.s.l. for PRS, 1 507 m for ZSF, 2 196 m for SNB and 1 231 m for CMN. These elevations are lower than those of the real stations, with differences ranging between 500 m (PRS) and 900–1 000 m (ZSF, SNB and CMN).

In the following sub–sections, the WRF trajectories that are connected to the exceptional CO_2 concentration values at the arrival sites are examined. The altitude of the trajectories has been analyzed focusing on their passage below an altitude of 1 500 m, where the air parcels could be eventually enriched with pollutants.

5.1. First event

The first event started at all the Alpine stations on 18 February (Figure 2). During the previous days, on 16 and 17 February, the WRF wind fields at 10 m above the surface and at pressure levels of between 1 000 and 700 hPa, were weak over central Europe and over northern and central Italy. All the 48–h three–dimensional backward trajectories that arrived at the PRS station on 17 February (not shown) always travelled at higher altitudes than 2 000 m a.s.l., with the exception of those at 00:00 UTC and 21:00 UTC, which were higher than 1 500 m a.s.l.

On 18 February, the WRF output emphasized the onset of northern winds over the central European plains in the parent grid and on the same day, the hourly CO_2 concentration increased at the 3 Alpine stations (beginning of the first event, Figure 2).

The event at the CMN station will be discussed later on because the CO_2 data (Figure 2c) show different behavior. In fact, the exact beginning of the event at the CMN station is unknown (no data are available between 08:00 UTC on 17 February and 02:00 UTC on 18 February), and the maximum seems to have occurred one day later. The air trajectories at this station are also very different from those that arrived at the Alpine stations.

On 18 February, the ZSF station measured increasing CO_2 values at 01:00 UTC, which SNB measured at 07:00 UTC and PRS at 13:00 UTC (Figure 2). The trajectories arriving at the three Alpine stations on 18 February changed in direction during the day (not shown). They were westerly in the first hours, and steadily became northerly from 18:00 UTC onwards.

The first relative CO_2 maxima were registered at the three stations at almost the same time in the evening when the trajectory arrived from the North (Figure 4a). The ZSF and SNB trajectories travelled for a long time at lower altitudes than 1 000 m a.s.l. and 1 500 m a.s.l. respectively, while the PRS trajectory always travelled above 2 000 m a.s.l.

According to WRF, on 19 February the wind strengthened and the trajectories were still from North to South with an anticyclonic curvature near the stations. At 06:00 UTC, when the PRS station measured the absolute maximum of CO_2, the PRS trajectory had been travelling for a long period in a layer between 500 m and 1 000 m a.s.l. (Figure 4b). Three hours later, at 09:00 UTC, when the maximum concentration of CO_2 was measured at the ZSF station, the arriving trajectory at the ZSF station had been under 500 m for 24 hours and under 1 000 m for another 24 hours (Figure 4c). The SNB station also measured a peak from 07:00 and 08:00 UTC and the SNB trajectories that arrived at 06:00 and 09:00 UTC showed that the direction had rotated anticlockwise from N to NW and that the altitude had decreased (Figures 4b and 4c). The trajectory at 09:00 UTC at PRS moved over central Europe to the eastern Alps at an altitude of about 2 000 m a.s.l. and then curved anticyclonically and travelled above the Po Valley at a lower layer than 1 500 m a.s.l. (Figure 4c). Three hours later, at 12:00 UTC, when the CO_2 concentration reached the third maximum, the PRS trajectory was almost the same (Figure 4d).

Since the three Alpine stations measured similar CO_2 concentration peaks at approximately the same time, and their associated trajectories moved over the same geographical area on the northern side of the Alps, the origin of the high concentration values was probably the same. In addition, the air mass that arrived at PRS could have been further enriched in CO_2 during its journey over the Po Valley.

In the hours following the CO_2 maxima, the wind remained intense, and the concentration values at the Alpine stations decreased. This could be explained by considering the effect of mixing and venting in the atmospheric boundary layer, which are favored by the presence of wind, even on the surface.

The first event at the CMN station was monitored with a delay of about one day. Since the CMN station did not collect data from 17 to 19 February, the exact onset time of the first event remains unknown (Figure 2c). The available data show that about 384 ppm was measured at 03:00 UTC on 19 February. The CO_2 concentration slowly increased, reaching values of between 387 and 389 ppm in the period between 16:00 UTC on 19 February and 12:00 UTC on 20 February (the maximum value was reached at 10:00 UTC). The trajectories that reached the CMN station on 19 February (Figure 4b–4d) came from the East, travelled at a low height and were not connected to the trajectories that arrived at the Alpine stations. The backward trajectories that arrived when the CO_2 concentrations reached their maximum values also travelled at a low height and arrived from the East. They crossed the Adriatic Sea and travelled over part of the Po Valley. So the high CO_2 values can be explained by the very low altitudes of the trajectories.

5.2. Second event

The two high CO_2 concentration events at PRS station were separated by a period of about two days (Figure 2). In the same days, the WRF outputs show that the winds on the surface and in the upper layers were weak over the plains (21 February) and then also over the Alps and Apennines (22 February). This fact is confirmed from the radio–soundings registered in Milan on 21 and 22 February, which were characterized by thermal inversions in the lowest layers of the atmosphere.

The second event started early in the morning on 23 February (Figure 2). At this time, the WRF simulation shows that northern winds were blowing over central Europe and over the Alpine region, whereas a surface wind was flowing over central Italy from the Southwest and crossing the whole peninsula.

The maximum CO_2 concentration occurred at the SNB station at 13:00 UTC and at the PRS station at 15:30 UTC (Figure 2b) whereas, due to a lack of measurements, it is not possible to recognize the maximum in the ZSF concentration values (Figure 2a). WRF computed an intense northern wind over the three Alpine stations in the central hours of the day.

The backward trajectories in Figure 5a represent the air parcel paths that arrived at the stations when the SNB station measured the maximum concentration. Both the SNB and ZSF trajectories came from North travelling winds at lower elevation than 1 000 m a.s.l., whereas the PRS trajectory arrived from the West, having travelled for a long period at lower altitudes than 500 m a.s.l.

Figure 5b shows the trajectories that arrived three hours later (at 15:00 UTC), when PRS showed the maximum CO_2 concentration. The PRS trajectory arrived after a long journey below 500 m a.s.l. in Northern Europe. A comparison with Figure 5a shows that the PRS trajectory completely changed direction, but remained below 500 m a.s.l. The SNB trajectory also arrived from the North, and travelled at about 1 000 m a.s.l. along most of its path. For this reason, the high CO_2 values observed in the SNB and PRS stations were probably due to transport from the lowest layers in the atmosphere. The ZFS trajectory also arrived from a northerly direction and its path had not changed significantly in the three previous hours. The decrease in CO_2 concentrations measured at the ZSF station in the morning could be explained by mixing in the atmospheric boundary layer.

The high concentration values at the Alpine stations registered for this event are therefore related to trajectories located in the lowest atmospheric layers.

As far as the CMN trajectories in Figure 5a and 5b are concerned, the air mass travelled over the Ligurian Sea at a higher altitude than 2 500 m a.s.l. and probably carried less CO_2. For this reason, the CMN station measured low concentrations when the Alpine stations measured relevant maxima. In the evening, the trajectory came from North Europe, circled the Alps on the French side, travelled over the Ligurian Sea and finally arrived at the CMN station (not shown). Some hours later, at 03:00 UTC on 24 February, the CMN trajectory crossed the Alps from North to South along the Canton Ticino (at about 46°N and 9°E) and travelled over the Po Valley at a low altitude under 500 m a.s.l. (Figure 5c). The CMN station registered the maximum values of CO_2 concentration at about 07:00 UTC on 24 February. The three–dimensional backward trajectory that crossed CMN at about that time (Figure 5d) came from the NE and was flowing at a low elevation over the eastern Po Valley. Therefore, in the morning of 24 February, the trajectories that arrived at CMN had travelled over the Po Valley from the N and NE at a low altitude.

In conclusion, the temporal evolution of the WRF wind fields on the surface and in the upper levels together with the trajectories suggest that, in both events, the air masses increased their CO_2 concentrations during their journey over the central Europe plains, and were carried southwards by the wind to the Alpine stations. During the first event, the air mass that arrived at PRS was also CO_2–enriched from high CO_2 values in the Po Valley, while, during the second event, the contribution in the Po Valley only influenced the measurements collected at the CMN station.

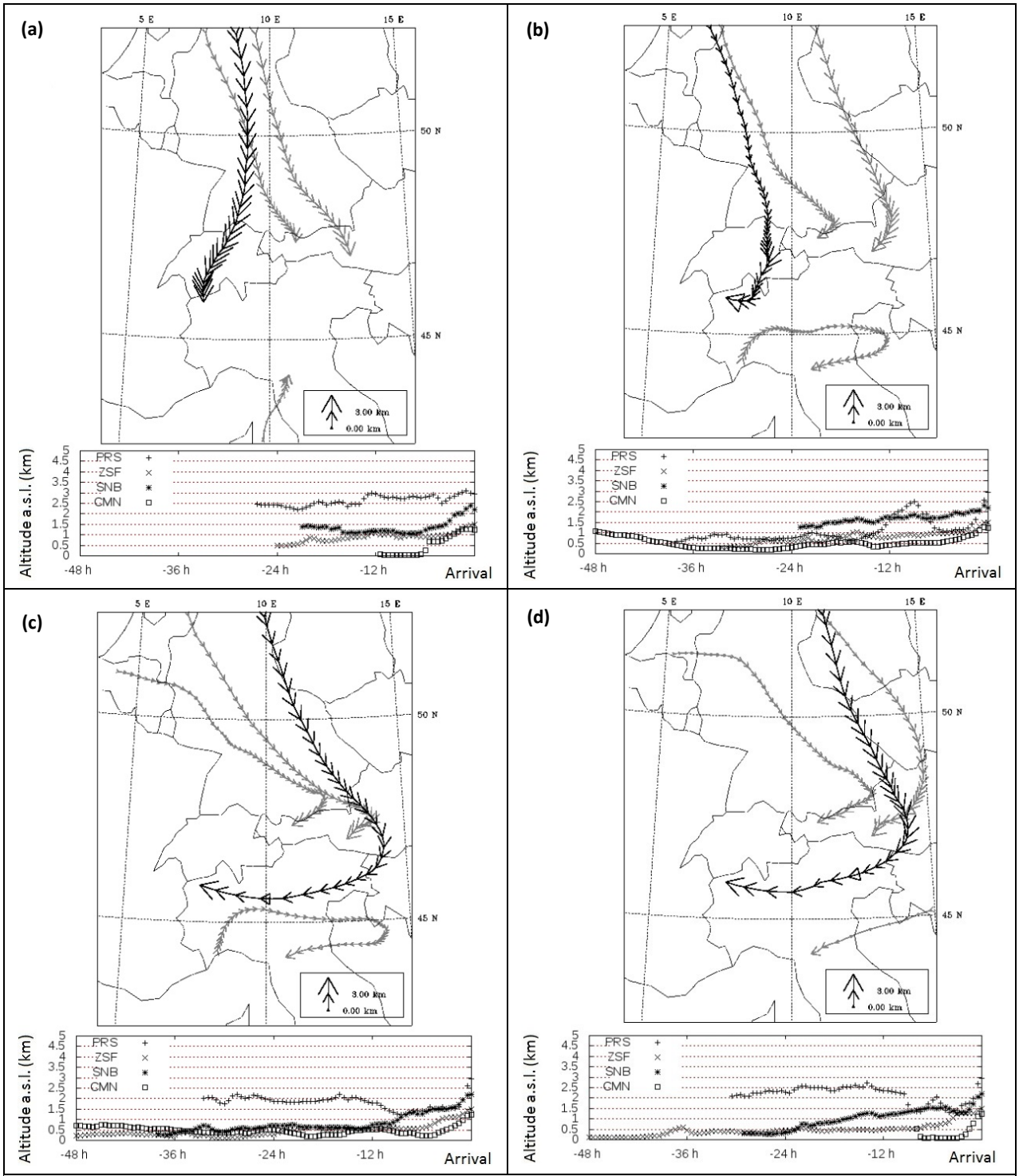

Figure 4. *The three–dimensional backward trajectories running in the inner domain and arriving at the four monitoring sites during the first event. The arrival time is 21:00 UTC on 18 February 2004* ***(a)****, 06:00 UTC on 19 February 2004* ***(b)****, 09:00 UTC on 19 February 2004* ***(c)****, and 12:00 UTC on 19 February 2004* ***(d)****. The size of the arrows (one each hour) in the horizontal plot is proportional to the altitude. The legend shows only three types of arrow: large (3.00 km level), medium (1.50 km level, not indicated) and small (similar to a point, at ground level). In the vertical sections, a.s.l. height (km) of the trajectories is plotted versus time (hours) with a point each half hour.*

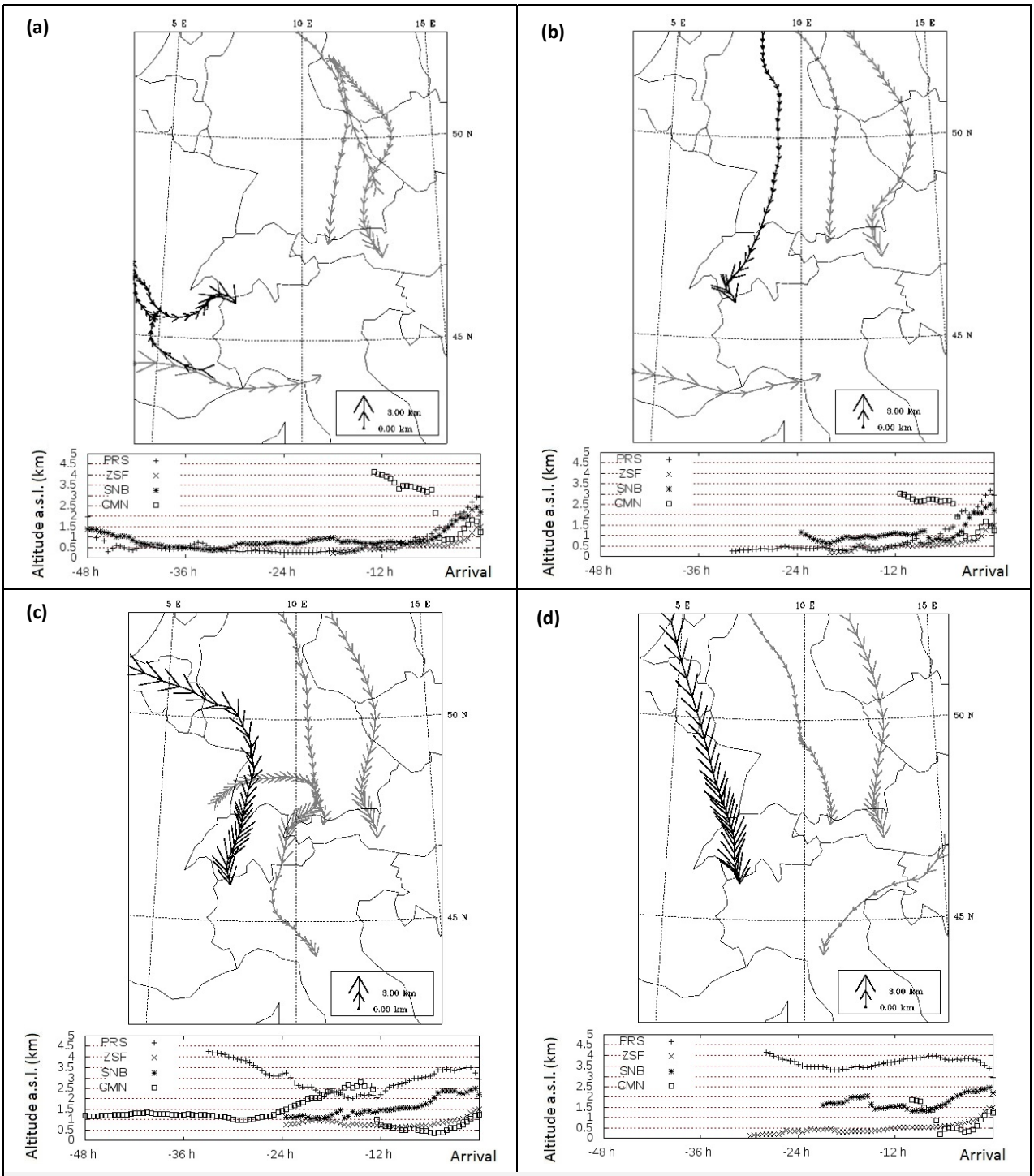

Figure 5. *The three–dimensional backward trajectories running in the inner domain and arriving at the four monitoring sites during the second event. The arrival time is 12:00 UTC on 23 February 2004* ***(a)****, 15:00 UTC on 23 February 2004* ***(b)****, 03:00 UTC on 24 February 2004* ***(c)*** *and 06:00 UTC on 24 February 2004* ***(d)****. The size of the arrows (one each hour) in the horizontal plot is proportional to the altitude. The legend shows only three types of arrow: large (3.00 km level), medium (1.50 km level, not indicated) and small (similar to a point, at ground level). In the vertical sections, a.s.l. height (km) of the trajectories is plotted versus time (hours) with a point each half hour.*

5.3. The CO and O_3 concentrations at the European stations

In order to confirm the previous conclusions about the CO_2 peaks, some tracers of human activity, such as CO and O_3, have been considered. Their concentration values were taken from the GAW database with reference to some Alpine stations in February 2004 (Figure 1 and Table 2).

Carbon monoxide is considered a quasi–conservative marker for anthropogenic pollutants in general (Parrish et al., 1998). Figure 6 compares the CO_2 concentration records at ZSF, PRS, SNB stations with the available CO records at Hohenpeissenberg (HPB, 42 km from ZSF, Table 2 and Figure 1), at Jungfraujoch (JFJ, 72 km from PRS, Table 2 and Figure 1) and at SNB itself, respectively. At SNB, where both CO and CO_2 were measured, a remarkable

coincidence of their peaks and similar trends are evident. The CO_2 record at PRS and the CO record at JFJ show similar trends and peaks, in spite of the distance between the stations. The agreement between CO_2 record at ZSF and the CO record at HPB is lower, because during the first event the CO peak is absent, and during the second the CO_2 peak was only partially detected due to the lack of data.

As regards the ozone, Figure 7 shows the O_3 concentrations at six stations in the northern side of the Alps (BRT and RIG stations, Table 2 and Figure 1 have been added to those mentioned above). In most of them the two events are characterized by a clear anti–correlation between O_3 and both CO_2 and CO concentrations, because minima of ozone concentration occur simultaneously to high–concentration CO_2 and CO maxima. The ozone minima are very pronounced at SNB and ZSF in both events and at the JFJ and RIG in the second one.

The tropospheric ozone concentration results from a complex combination of production, transport, chemical destruction and deposition. Tropospheric ozone has several well documented sources, natural and anthropogenic: download transport from the stratosphere, local photochemical production from precursors (volatile organic compounds (VOCs), carbon monoxide (CO) and nitrogen oxides (NO_x), remote production associated with long–range transport (Chevalier et al., 2007).

Table 2. *GAW stations in the Alpine area measuring CO and O_3 concentration in February 2004*

Station	GAW_ID	Altitude (m a.s.l.)	Available Data
Brotjacklriegel	BRT	1 016	O_3
Hohenpeissenberg	HPB	985	O_3 and CO
Jungfraujoch	JFJ	3 580	O_3 and CO
Rigi	RIG	1 031	O_3
Sonnblick	SNB	3 106	O_3 and CO
Zugspitze–Schneefernerhaus	ZSF	2 656	O_3

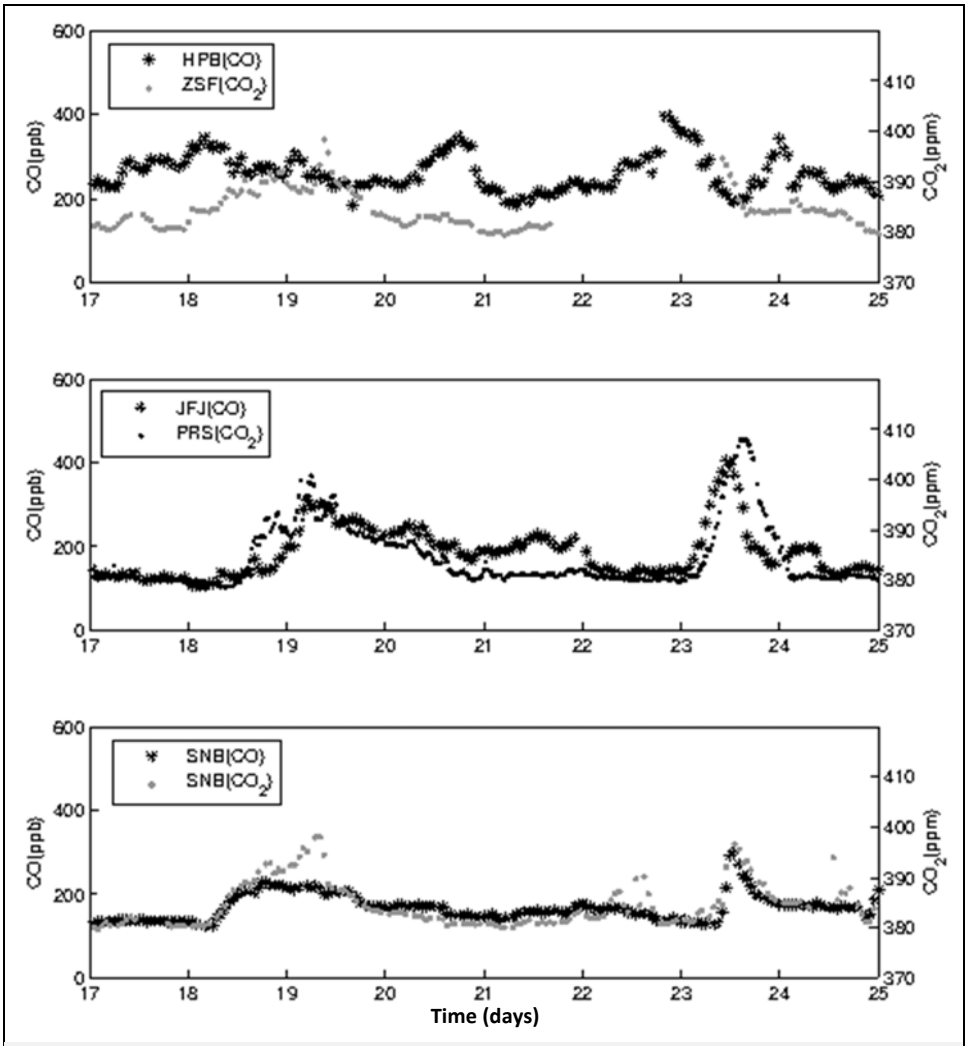

Figure 6. *CO concentrations (ppb) measured from 17 to 25 February 2004 at the HPB, JFJ and SNB stations (left scale), and CO_2 concentrations (ppm) at the nearby ZSF, PRS and SNB itself stations, respectively (right scale).*

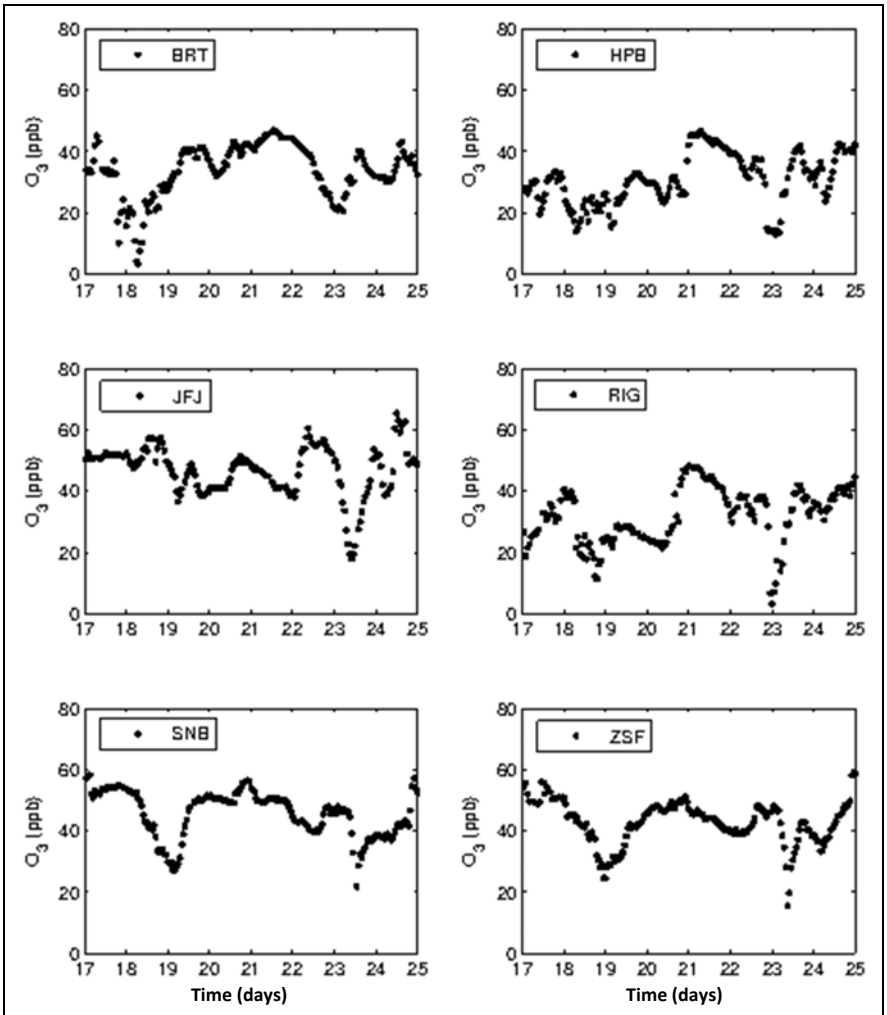

Figure 7. *O_3 concentrations (ppb) measured from 17 to 25 February 2004 at the BRT, HPB, JFJ, RIG, SNB and ZSF stations.*

At mountain stations in central Europe ozone concentration shows an annual cycle with summer maxima and winter minima. Only in summer the boundary layer net photochemical ozone production is linked to regional anthropogenic emission, in other seasons anthropogenic emission tend to suppress ambient ozone (Gilge et al., 2010). At Alpine stations a weekly cycle with lower O_3 concentrations during working days and maxima on the weekend in autumn and winter is observed, implying an anti–correlation between O_3 and the anthropogenic pollutant during the cold season (Gilge et al., 2010). The anti–correlation is also observed during wintertime pollution events as described by Parrish et al. (1998). Both Gilge et al. (2010) and Parrish et al. (1998) ascribe the cause of this negative correlation to the removal of ozone by the reaction with anthropogenic pollutant (titration by NO). Therefore, the anti–correlation between O_3 and both CO_2 and CO concentrations that occurred during the two events of February 2014 strongly supports the hypothesis that the high CO_2 concentration values were caused by the advection of polluted air from the atmospheric boundary layer.

6. Conclusions

Two events of high CO_2 concentration that occurred few days apart at the Plateau Rosa station have been investigated. They can be considered exceptional, because during these events the daily mean values exceeded the corresponding monthly averages by six standard deviations derived from a 21–years statistics. Similar and almost contemporary maxima, even though statistically not exceptional, were also measured at the Zugspitze–Schneefernerhaus and Sonnblick Alpine stations and at the Apennine Mt. Cimone station.

A numerical simulation was performed using the WRF meteorological model in order to compute the high resolution wind fields. The setup included a 7 km resolution grid, nested in a parent 21 km resolution grid. Three–dimensional two–day–long backward trajectories from the four stations were calculated from the WRF wind fields.

The backward trajectories show that, during the first event, the three Alpine stations were reached by air masses from North European plains and that travelled at a low altitude. In particular, the Plateau Rosa station was initially crossed by trajectories from the North and, at the end of the episode, the air mass that reached the Plateau Rosa station outflanked the eastern side Alps and moved above the Po Valley. The Mt. Cimone station measured a CO_2 concentration peak with a delay of several hours, and the associated trajectories, driven by eastern winds, are unconnected to the trajectories that arrived at the Alpine station. Their low altitude could explain the high measured CO_2 values.

During the second event, the wind again flew from the northern sectors and reached the Alpine stations without travelling

over the Po Valley. Again in this case, the air parcels travelled at a low altitude over the European plains before arriving at the monitoring station. The north–eastern air mass reached Mt. Cimone only 16 hours later, when the flow was able to take the air mass above the lower Po Valley, after having crossed the Alps.

The contamination of the air masses by anthropogenic pollution episodes has been confirmed through an analysis of the short–lived gas concentrations (carbon monoxide and ozone) recorded at several GAW stations in the Alps. It appears therefore that the two high CO_2 concentration events measured at the three high–mountain stations in the Alps were caused by the transport of an air mass that was enriched in CO_2 during its journey in the atmospheric boundary layer over the plains. The synoptic configuration favored the permanence of the air masses above the plains for several consecutive days before the episodes, and contributed to the enrichment of the CO_2 concentration. A new circulation then transported these polluted air masses above the three monitoring stations, and caused a rapid increment in the concentration. Statistical analysis over the 21–years Plateau Rosa series showed that these events occur more frequently during the cold season.

It is possible to conclude that even remote, very high mountain stations can occasionally measure very high CO_2 concentration peaks when the flow patterns are able to convey polluted air masses from the plains to the mountains. In highly complex sites like the Alps, a detailed analysis of atmospheric circulation and the use of a high resolution regional meteorological model come out essential to study this kind of events.

Acknowledgments

This work has partially been founded by the Research Fund for the Italian Electrical System under the Contract Agreement between RSE (formerly known as ERSE) and the Ministry of Economic Development–General Directorate for Nuclear Energy, Renewable Energy and Energy Efficiency stipulated on July 29, 2009 in compliance with the Decree of March 19, 2009. The authors would like to thank both the GAW (http://www.wmo.int/gaw/) organization and the PIs of the monitoring stations (Ludwig Ries from Zugspitze–Schneefernerhaus, Marina Frohlich and Gerhard Schauer from Sonnblick and, Attilio Di Diodato and Marco Alemanno from Mt. Cimone) for providing the CO_2 concentration data.

Supporting Material Available

Historical series of the monthly CO_2 background concentrations at Plateau Rosa site (Figure S1), meteorological surface maps (Figure S2), comparison between modelled and observed vertical profile on southern side of the Alps (Figure S3), and on northern side of the Alps (Figure S4). This information is available free of charge via the Internet at http://www.atmospolres.com.

References

Apadula, F., Gotti, A., Pigini, A., Longhetto, A., Rocchetti, F., Cassardo, C., Ferrarese, S., Forza, R., 2003. Localization of source and sink regions of carbon dioxide through the method of the synoptic air trajectory statistics. *Atmospheric Environment* 37, 3757–3770.

Bousquet, P., Peylin, P., Ciais, P., Le Quere, C., Friedlingstein, P., Tans, P.P., 2000. Regional changes in carbon dioxide fluxes of land and oceans since 1980. *Science* 290, 1342–1346.

Bowman, K.P., Lin, J.C., Stohl, A., Draxler, R., Konopka, P., Andrews, A., Brunner, D., 2013. Input data requirements for Lagrangian trajectory models. *Bulletin of the American Meteorological Society* 94, 1051–1058.

Chevalier, A., Gheusi, F., Delmas, R., Ordóñez, C., Sarrat, C., Zbinden, R., Thouret, V., Athier, G., Cousin, J.M., 2007. Influence of altitude on ozone levels and variability in the lower troposphere: a ground-based study for western Europe over the period 2001-2004. *Atmospheric Chemistry and Physics* 7, 4311-4326.

Conway, T.J., Tans, P., Waterman, L.S., Thoning, K.W., Masarie, K.A., Gammon, R.H., 1988. Atmospheric carbon dioxide measurements in the remote global troposphere, 1981–1984. *Tellus Series B–Chemical and Physical Meteorology* 40B, 81–115.

Conway, T.J., Tans, P.P., Waterman, L.S., Thoning, K.W., 1994. Evidence for interannual variability of the carbon cycle from the National Oceanic and Atmospheric Administration/Climate Monitoring and Diagnostics Laboratory Global Air Sampling Network. *Journal of Geophysical Research–Atmospheres* 99, 22831–22855.

Ferrarese, S., Longhetto, A., Cassardo, C., Apadula, F., Bertoni, D., Giraud, C., Gotti, A., 2002. A study of seasonal and yearly modulation of carbon dioxide sources and sinks, with a particular attention to the Boreal Atlantic Ocean. *Atmospheric Environment* 36, 5517–5526.

Forster, P., Ramaswamy, V., Artaxo, P., Berntsen, T., Betts, R., Fahey, D.W., Haywood, J., Lean, J., Lowe, D.C., Myhre, G., Nganga, J., Prinn, R., Raga, G., Schulz, M., Van Dorland, R., 2007. Changes in atmospheric constituents and in radiative forcing, *in Climate Change 2007: The Physical Science Basis*, Contribution of Working Group I to the Fourth Assessment Report of the Intergovernmental Panel on Climate Change*, edited by* Solomon, S., Qin, D., Manning, M., Chen, Z., Marquis, M., Averyt, K.B., Tignor M., Miller, H.L., Cambridge University Press*,* Cambridge and New York, pp. 129–234.

Geels, C., Gloor, M., Ciais, P., Bousquet, P., Peylin, P., Vermeulen, A.T., Dargaville, R., Aalto, T., Brandt, J., Christensen, J.H., Frohn, L.M., Haszpra, L., Karstens, U., Rodenbeck, C., Ramonet, M., Carboni, G., Santaguida, R., 2007. Comparing atmospheric transport models for future regional inversions over Europe – Part 1: Mapping the atmospheric CO_2 signals. *Atmospheric Chemistry and Physics* 7, 3461–3479.

Gilge, S., Plass–Duelmer, C., Fricke, W., Kaiser, A., Ries, L., Buchmann, B., Steinbacher, M., 2010. Ozone, carbon monoxide and nitrogen oxides time series at four Alpine GAW mountain stations in central Europe. *Atmospheric Chemistry and Physics* 10, 12295–12316.

Gohm, A., Harnisch, F., Vergeiner, J., Obleitner, F., Schnitzhofer, R., Hansel, A., Fix, A., Neininger, B., Emeis, S., Schafer, K., 2009. Air pollution transport in an Alpine Valley: Results from airborne and ground–based observations. *Boundary–Layer Meteorology* 131, 441–463.

Henne, S., Furger, M., Prevot, A.S.H., 2005a. Climatology of mountain venting–induced elevated moisture layers in the lee of the Alps. *Journal of Applied Meteorology* 44, 620–633.

Henne, S., Dommen, J., Neininger, B., Reimann, S., Staehelin, J., Prevot, A.S.H., 2005b. Influence of mountain venting in the Alps on the ozone chemistry of the lower free troposphere and the European pollution export. *Journal of Geophysical Research–Atmospheres* 110, art. no. D22307.

Henne, S., Furger, M., Nyeki, S., Steinbacher, M., Neininger, B., de Wekker, S.F.J., Dommen, J., Spichtinger, N., Stohl, A., Prevot, A.S.H., 2004. Quantification of topographic venting of boundary layer air to the free troposphere. *Atmospheric Chemistry and Physics* 4, 497–509.

Kaiser, A., Scheifinger, H., Spangl, W., Weiss, A., Gilge, S., Fricke, W., Ries, L., Cemas, D., Jesenovec, B., 2007. Transport of nitrogen oxides, carbon monoxide and ozone to the Alpine Global Atmosphere Watch stations Jungfraujoch (Switzerland), Zugspitze and Hohenpeissenberg (Germany), Sonnblick (Austria) and Mt. Krvavec (Slovenia). *Atmospheric Environment* 41, 9273–9287.

Keeling, R.F., 2008. Recording Earth's vital signs. *Science* 319, 1771–1772.

Keeling, C.D., Bacastow, R.B., Bainbridge, A.E., Ekdahl, C.A., Guenther, P.R., Waterman, L.S., Chin, J.F.S., 1976. Atmospheric carbon dioxide variations at Mauna Loa Observatory, Hawaii. *Tellus* 28, 538–551.

Kossmann, M., Corsmeier, U., De Wekker, S., Fiedler, F., Vogtlin, R., Kalthoff, N., Gusten, H., Neininger, B., 1999. Observations of handover processes between the atmospheric boundary layer and the free troposphere over mountainous terrain. *Contributions to Atmospheric Physics* 72, 329–350.

Lashof, D.A., Ahuja, D.R., 1990. Relative contributions of greenhouse gas emissions to global warming. *Nature* 344, 529–531.

Longhetto, A., Ferrarese, S., Cassardo, C., Giraud, C., Apadula, F., Bacci, P., Bonelli, P., Marzorati, A., 1997. Relationships between atmospheric circulation patterns and CO_2 greenhouse–gas concentration levels in the Alpine troposphere. *Advances in Atmospheric Sciences* 14, 309–322.

Longhetto, A., Apadula, F., Bacci, P., Bonelli, P., Cassardo, C., Ferrarese, S., Giraud, C., Vannini, C., 1995. A study of greenhouse gases and air trajectories at Plateau Rosa. *Nuovo Cimento Della Societa Italiana Di Fisica C–Geophysics and Space Physics* 18, 583–601.

Loov, J.M.B., Henne, S., Legreid, G., Staehelin, J., Reimann, S., Prevot, A.S.H., Steinbacher, M., Vollmer, M.K., 2008. Estimation of background concentrations of trace gases at the Swiss Alpine site Jungfraujoch (3 580 m asl). *Journal of Geophysical Research–Atmospheres* 113, art. no. D22305.

Masarie, K.A., Tans, P.P., 1995. Extension and integration of atmospheric carbon dioxide data into a globally consistent measurement record. *Journal of Geophysical Research: Atmospheres* 100, 11593–11610.

Mastrangelo, D., Horvath, K., Riccio, A., Miglietta, M.M., 2011. Mechanisms for convection development in a long–lasting heavy precipitation event over Southeastern Italy. *Atmospheric Research* 100, 586–602.

Miglietta, M.M., Zecchetto, S., De Biasio, F., 2013. A comparison of WRF model simulations with SAR wind data in two case studies of orographic lee waves over the Eastern Mediterranean Sea. *Atmospheric Research* 120, 127–146.

Miglietta, M.M., Moscatello, A., Conte, D., Mannarini, G., Lacorata, G., Rotunno, R., 2011. Numerical analysis of a Mediterranean 'hurricane' over South–Eastern Italy: Sensitivity experiments to sea surface temperature. *Atmospheric Research* 101, 412–426.

Papanastasiou, D.K., Melas, D., Lissaridis, I., 2010. Study of wind field under sea breeze conditions; an application of WRF model. *Atmospheric Research* 98, 102–117.

Parrish, D.D., Trainer, M., Holloway, J.S., Yee, J.E., Warshawsky, M.S., Fehsenfeld, F.C., Forbes, G.L., Moody, J.L., 1998. Relationships between ozone and carbon monoxide at surface sites in the North Atlantic region. *Journal of Geophysical Research–Atmospheres* 103, 13357–13376.

Peters, W., Krol, M.C., van der Werf, G.R., Houweling, S., Jones, C.D., Hughes, J., Schaefer, K., Masarie, K.A., Jacobson, A.R., Miller, J.B., Cho, C.H., Ramonet, M., Schmidt, M., Ciattaglia, L., Apadula, F., Helta, D., Meinhardt, F., di Sarra, A.G., Piacentino, S., Sferlazzo, D., Aalto, T., Hatakka, J., Strom, J., Haszpra, L., Meijer, H.A.J., van der Laan, S., Neubert, R.E.M., Jordan, A., Rodo, X., Morgui, J.A., Vermeulen, A.T., Popa, E., Rozanski, K., Zimnoch, M., Manning, A.C., Leuenberger, M., Uglietti, C., Dolman, A.J., Ciais, P., Heimann, M., Tans, P.P., 2010. Seven years of recent European net terrestrial carbon dioxide exchange constrained by atmospheric observations. *Global Change Biology* 16, 1317–1337.

Ramonet, M., Ciais, P., Aalto, T., Aulagnier, C., Chevallier, F., Cipriano, D., Conway, T.J., Haszpra, L., Kazan, V., Meinhardt, F., Paris, J.D., Schmidt, M., Simmonds, P., Xueref–Remy, I., Necki, J.N., 2010. A recent build–up of atmospheric CO_2 over Europe. Part 1: Observed signals and possible explanations. *Tellus Series B–Chemical and Physical Meteorology* 62, 1–13.

Rodenbeck, C., Houweling, S., Gloor, M., Heimann, M., 2003. CO_2 flux history 1982–2001 inferred from atmospheric data using a global inversion of atmospheric transport. *Atmospheric Chemistry and Physics.* 3, 1919–1964.

Schoner, W., Bohm, R., Auer, I., 2012. 125 years of high–mountain research at Sonnblick Observatory (Austrian Alps) – from "the house above the clouds" to a unique research platform. *Theoretical and Applied Climatology* 110, 491–498.

Skamarock, W.C., Klemp, J.B., Dudhia, J., Gill, D.O., Barker, D.M., Duda, M.G., Huang, X., Wang, W., Powers, J.G., 2008. *A Description of the Advanced Research WRF Version 3*, NCAR Technical Note, Boulder, USA, 125 pages.

Stoelinga, M.T., 2009. A Users' Guide to RIP Version 4.5: A Program for Visualizing Mesoscale Model Output. http://www.mmm.ucar.edu/wrf/users/docs/ripug.htm, accessed in November 2014.

Tans, P.P., Conway, T.J., Nakazawa, T., 1989. Latitudinal distribution of the sources and sinks of atmospheric carbon–dioxide derived from surface observations and an atmospheric transport model. *Journal of Geophysical Research–Atmospheres* 94, 5151–5172.

Trapero, L., Bech, J., Lorente, J., 2013. Numerical modelling of heavy precipitation events over Eastern Pyrenees: Analysis of orographic effects. *Atmospheric Research* 123, 368–383.

Trusilova, K., Rodenbeck, C., Gerbig, C., Heimann, M., 2010. Technical note: A new coupled system for global to regional downscaling of CO_2 concentration estimation. *Atmospheric Chemistry and Physics* 10, 3205–3213.

Uglietti, C., Leuenberger, M., Brunner, D., 2011. European source and sink areas of CO_2 retrieved from Lagrangian transport model interpretation of combined O_2 and CO_2 measurements at the high alpine research station Jungfraujoch. *Atmospheric Chemistry and Physics.* 11, 8017–8036.

Wada, A., Sawa, Y., Matsueda, H., Taguchi, S., Murayama, S., Okubo, S., Tsutsumi, Y., 2007. Influence of continental air mass transport on atmospheric CO_2 in the Western North Pacific. *Journal of Geophysical Research–Atmospheres* 112, art. no. D07311.

Weigel, A.P., Chow, F.K., Rotach, M.W., 2007. The effect of mountain topography on moisture exchange between the "surface" and the free atmosphere. *Boundary Layer Meteorology* 125, 227–244.

WDCGG, 2014. http://ds.data.jma.go.jp/gmd/wdcgg/, accessed in October 2014.

WMO, 2009. Technical Report of Global Analysis Method for Major Greenhouse Gases by the World Data Center for Greenhouse Gases, GAW Report No.184 (WMO TD No. 1473), Geneva, 29 pages.

WMO Greenhouse Gas Bulletin, 2013. The State of Greenhouse Gases in the Atmosphere Based on Global Observations Through 2012, No.9, Geneva, 4 pages.

Wotawa, G., Kroger, H., Stohl, A., 2000. Transport of ozone towards the Alps – Results from trajectory analyses and photochemical model studies. *Atmospheric Environment* 34, 1367–1377.